ORIGINAL ARTICLE

RECORDS OF PHARMACEUTICAL AND BIOMEDICAL SCIENCES

Contribution in the Quality Assessment of Myrrh

Yomna Abdelrahman[a], Reham S. Ibrahim[b], Hoda Fathy[*b] and Mohamed I. Aboushoer[b]

[a]Department of Pharmacognosy, Faculty of Pharmacy and drug manufacturing, Pharos university, Alexandria, Egypt; [b]Department of Pharmacognosy, Faculty of Pharmacy, Alexandria University, Alexandria, Egypt;

Received on: 21-05-2024

Revised on: 11-06-2024

Accepted on: 14-06-2024

*Correspondence Author:

Phone: 00201001223411

E-mail:

hoda.sherif@alexu.edu.eg,

hodasherif@hotmail.com,

https://orcid.org/0000-0002-8268-0569

Abstract

Myrrh was used anciently in difficult cultures as in embalming fluids by Egyptians, in Chinese and other traditional medicine. However, research about activity of myrrh till now is not very convincing. Compendial description of myrrh wasn't helpful nor convenient in fully describing the composition as well as the attributes of the nature of myrrh, which put a burden on healthcare providers to appropriately prescribe it as it lacks the adequate validation tool in its healing properties or practices. Methods used were descriptive parameters, such as color and particle size. Furthermore, we enforced chemical instrumental procedures, such as near infrared spectra, Thin layer chromatography and ultraviolet spectroscopy profiling. In conclusion, in vitro biological α-glucosidase activity of myrrh was assigned. Impartially, NIR spectra of Myrrh were recorded and attempt to assign peaks of myrrh's chemical composition, this is the first study to use this approach for myrrh. Particle size and color-PLS models with low RMSEC and RMSECV was useful to estimate alpha-glucosidase inhibitory activity with acceptable accuracy. In the absence of evidence based therapeutic indication for myrrh chemistry we must accurately study the composition of myrrh and agree upon species.

Keywords: Myrrh quality; near infrared; RGB, alpha-glucosidase inhibition, PLS.

1. Introduction:

Myrrh, is widely known for its use as incense in religious rituals. Formerly, it was a highly valuable commodity in trade. Myrrh is an oleo gum resin collected in summer from cracks; made naturally or intentionally; into the bark of *Commiphora* species belonging to family Burseraceae. Both the European Pharmacopoeia (Ph.Eur 7.0) and the United States Pharmacopeia (USP 34) define myrrh as the gum-resin obtained from the stems and branches of *C. molmol* among many other related species of *Commiphora*. B. Somalia and Ethiopia are by far the largest producers of this resin (Miller & Goodell, 1968). Moreover, it is approved by the Food and Drug Administration (FDA) as a food additive and listed as GRAS (Generally Recognized as Safe). Extract of myrrh is also approved by Commision E for its antibacterial and astringent properties. Assimopoulou A.N. and Hamad GM recommended its addition to yogurt or milk as a functional food which has antioxidant activity and help aid in preventing colon cancer in humans.(Assimopoulou et al., 2005; Hamad et al., 2017).

Myrrh as a complementary medicine has wide range of activity as antifungal, antibacterial, expectorant and antiviral (Chandrasekharnath et al., 2013; Shameem & Fahad, 2018). It is used in addition to other herbs as a remedy for some covid-19 symptoms (Alyafei, 2020). It is assumed that the extract of myrrh has a cytotoxic activity in breast and prostate cancer in-vivo on mice (Cao et al., 2019).

Several experimental and clinical studies locally have been published to investigate the effect of Myrrh extracts on different types of parasites, especially *Schistosoma* and *Fasciola*. Their results were controversial, many of them affirms its effectiveness compared with the synthetic drug praziquantel (Massoud et al., 2010) especially in the recommended daily doses (Barakat et al., 2005).

Chemically, Myrrh is an oleo gum resin; gum which is mainly polysaccharides, proteins and oxidase enzyme represents 40-60% and is water soluble while the resin which represents 20-40% and the volatile oil fractions are alcohol soluble (Hanuš et al., 2005).

Being a non-herbal medicine, it represents a challenge in its quality control due to its huge number of constituents most of which are of complicated structure. Even though, NIR is not a common analytical method. However, currently it has a wide application in identification and authentication of many natural products and raw materials,

Images showing gross features of myrrh can be captured by a simple smart phone as a rapid, real-time detection with acceptable accuracy, can be used through Digital image analysis using Red- Green -Blue (RGB) method to evaluate samples' variability.

The significant global market demand of myrrh requires vigilance in assigning the quality of myrrh

The safety claims and therapeutic indications are crucial to predict any hurdles or health care problems that might be associated due to missing specifications and/or quality markers.

For the above-mentioned ambiguity, the authors of this work have imperatively felt that it is necessary to conduct this research. The study in hand describes a feasible methodology to assess whether the marketed myrrh is appropriate for its designed aspects and attributes. Meanwhile, work was attempted without resorting to sophisticated analytical techniques due to the complex-nature of the resin.

2. Materials and Methods:

2.1. Myrrh samples acquisition

Fifteen different myrrh oleo gum resin samples were purchased locally and other from different countries according to the current national guidelines. Sample's claimed origin were from Yemen /Hadramout (1sample (1s)), South Africa (1s), Morocco (1s), Somalia (4s), Sudan (5s), Saudi Arabia (2s) and unknown (3s). For details of each sample origin, purchase place and price, refer to supplementary materials (Table 1).

2.2. Obtention and treatment of digital images of myrrh samples and sample solutions

Standardized image procedures were developed to capture similarity and differences between the samples as a raw material.

This was repeated though for the methanolic solution of the 15 myrrh samples and image captured was processed using imagej software where intensity as well as the mean value of the colors' components (RGB) were measured.

Another approach was applied to samples` raw material which was particle size measurement, to assess the observed differences in sizes and shape.

2.2.1. Crude samples' images

Few representative particles of each sample were placed in an area of approximately 3cm*3 cm over a large white canson sheet. Iphone 11 pro 12 mega pixels camera was employed to capture the samples under white light, the sample-camera distance was kept constant to ensure reproducibility of the measurements. Then, the images were exported to Imagej software 1.47b/ Java 1.6.0_12 (64-bit) image processing program or Adobe photoshop CC 2018.

The mean value for each of the property of red, green and blue color components, as well as the intensity were calculated by the software, recorded and then arranged in a matrix.

2.2.2. Samples solutions' images

Representative 1 g from each of the 15 samples were dissolved in 5ml methanol and placed in vials of the same size, then captured in one image to ensure that they were all subjected to the same conditions. Then, a fixed-size square window for each vial was maintained throughout the analysis via imagej software.

2.2.3. Average particle length determination

For particle length determination, the same images captured in the previous section were also imported to ImageJ software. Line tool selected from the tool bar used to draw a straight line along the length of the scale bar (1 cm previously drawn in the image) as precise as possible to be used as a standard to set the measurements. Manual measuring was carried thrice in different directions using the line tool for each of the seven particles then the average was calculated.

The length of each sample was calculated from the average of 7 particles.

Table 1. Samples' codes according to their claimed origin and country purchased from

code	purchased from	Claimed source of cultivation	average of particles length	Price / kilo	Date of purchase	Amount purchased
M-1	Saudi Arabia /Jeddah	Yemen	3.39	300 S.R=1283 L.E	2019	500 gm
M-2	Egypt /Luxor	South Africa	Average of large pieces 4.88 Average of small pieces 0.89	750 L.E	2020	250 gm
M-3	Saudi Arabia /Jeddah	Somalia	3.0347	600 L.E	2019	250 gm
M-4	Egypt /Cairo	Somalia	2.76	700 L.E	2019	500 gm
M-5	Bahrain	Somalia	0.95	1500 L.E	2019	100 gm
M-6	Kuwait	Somalia	1.44	1500 L.E	2019	50 gm
M-7	Egypt /Cairo	Morocco	1.69	1000 LE	2019	250 gm
M-8	Kuwait	Sudan	0.85	1600 LE	2019	500 gm
M-9	Egypt /Luxor	Sudan	2.05	800 L.E	2019	125 gm
M-10	Egypt /Luxor	Sudan	2.44	700 L.E	2019	125 gm
M-11	Egypt /Luxor	Sudan	0.55	700 L.E	2020	125 gm
M-12	Egypt /Luxor	Sudan	7.04	800 L.E	2020	125 gm
M-13	Kuwait	Saudi Arabia	1.92	1500 L.E	2021	125 gm
M-14	Kuwait	Saudi Arabia	0.96	1500 L.E	2021	125 gm
M-15	Bahrain	unknown	1.47	1500 L.E	2021	125 gm
M-16	Egypt	unknown	0.52	Obtained from department	2015	125 gm
M-17	Saudi Arabia	unknown	0.66	Obtained from department	1980	20 gm

2.3. Chromatographic and spectral analysis

chromatographic and spectroscopic techniques were applied, such as High-Performance Thin Layer Chromatography (HPTLC), UV spectroscopy and Near Infrared data (NIR) spectroscopy.

2.3.1. High Performance Thin Layer Chromatography (HPTLC)

Application was performed on precoated HPTLC silica gel plates (GF-254 Merck, Darmstadt, Germany) by means of Camag Linomat IV automated spray-on band applicator equipped with a 100 µl Hamilton syringe using constant application rate. The application position was set at 10 mm from the bottom and from each side with a 6 mm band width and 4 mm distance between bands. Sample application volume was set to 8 µl. The plate was developed for 80 mm distance in (Camag) twin trough chromatographic chamber saturated for 15 min with the vapors of mobile phase Toluene : ethanol: acetic acid 97:3:0.1 v/v/v. before the run, air dried , sprayed with methanol sulphuric acid 10 % sulfuric acid in methanol and visualized under UV lamp at λ 366 nm. 0.5 ml Anisaldehyde was mixed with 10 ml glacial acetic acid, followed by 85 ml methanol, the mixture was cooled then 5 ml concentrated sulfuric acid were added slowly.

2.3.2. TLC- Image analysis

Image processing was carried out using several approaches:

-Sorbfil TLC image was captured, stored as JPEG, the image was opened in Sorbfil TLC Video densitometer, a program elaborated by Sorbpolymer JSC (Krasnodar, Russian Federation), and analyzed using the track command evaluation for each track.

-Imagej

TLC plate image saved as jpg files converted into 8 bite and data was obtained using imagej software. Data was detached and divided into 3 readings according to color red, green and blue channels.

Another approach using the imagej software was by using a fixed rectangular marker for each spot on the 15 track and measuring the intensity of each spot using the RGB colors as previous.

2.3.3. UV spectroscopy:

One gram of each myrrh samples was extracted with 10 mL methanol using ultrasound assisted extraction (USAE), filtered and volume adjusted. Measured on UV-Visible spectrophotometer equipment (Perkin Elmer® UV/VIS spectrometer (Singapore) with double beam). medium wavelength speed scanning, supported

with UV Win Lab™ software, using 1 cm bath length quartz cuvette cells. The raw spectral UV data matrix of all the samples were mean centered, which is the default option applied to the software. Freshly prepared aluminum chloride was used as shifts reagents. • Freshly prepared aluminum chloride Anhydrous AlCl3 (5g) was cautiously dissolved in 100 ml. spectroscopic methanol and filtration was carried out then stored in the fridge, and no bathochromic shift was observed.

2.3.4. Near Infrared data (NIR) spectroscopy

The grounded samples' spectra were scanned using multi-purpose analyzer (MPA) Fourier Transform Near Infra-Red (FT-NIR) spectrometer (Bruker Optics GmbH, Ettlingen, Germany) with an integrating sphere module and InGaAs linear photodiode array detector over the wavenumbers 8000–4000 cm^{-1}. The spectra were then acquired with the OPUS software (ver. 6.5, Bruker Optics Inc.) at a resolution of 16 cm^{-1} per spectrum by taking the mean of over 64 scans. Each sample was measured in triplicate, and the mean spectrum was considered in order to reduce the noise due to instrument. A uniform glass vessel (diameter = 20 mm, height = 50 mm) to load the samples (approximately 1 g of powder to cover the bottom) was utilized to reduce the error of operation.

2.4. In vitro biological activity evaluation

2.4.1. In vitro α-glucosidase inhibitory activity assay

In 96-well plate, 50 µl of myrrh extract at 500 µl /ml concentration was added to 10 µl of α glucosidase enzyme (E.C. 3.2.1.20) and 125 µl of 0.1M phosphate buffer (pH 6.8). The reaction mixture is then preincubated at 37°C for 20 min.

After preincubation, 20 µL of the substrate 1M p-nitrophenyl-α-D-glucopyranoside (pNPG) and the mixture was incubated for 30 min. at 37°C. Then, 100 µl Na_2CO_3 (200 mM) is added to each well to terminate the reaction. The absorbance was measured at 410 nm. The blank sample wells contain phosphate buffer instead of *α*-glucosidase and inhibitor.

The control sample wells contain phosphate buffer instead of inhibitor sample. Acarbose is used as a standard inhibitor (positive control) at different concentrations.

Enzyme activity was calculated as:

% Inhibition = [(OD CONTROL-OD SAMPLE)/OD CONTROL] x 100

One unit of the enzyme can be defined as the amount of enzyme (α-glucosidase) required for the formation of one µmol of product (p-Nitrophenol) from the substrate (p-nitrophenyl-α-D-glucopyranoside) per minute.

2.4.2. In vitro pancreatic lipase inhibitory assay

500 µg/ml myrrh solution in 10% DMSO was used, 1 mg/ml stock solution of pancreatic lipase enzyme was prepared immediately before being used. A stock solution of p-NPB was prepared by dissolving 20.9 mg of p-NPB in 2 ml of acetonitrile. 0.1 ml of porcine pancreatic lipase (1 mg/ml) was added to test tubes containing 0.2 ml of the previously prepared myrrh solution. The resulting mixtures were then made up to 1 ml by adding Tri-HCl solution (pH 7.4) and incubated at 25 °C for 15 min. After the incubation period, 0.1 ml of p-NPB solution was then added to each test tube. The mixture was again incubated for 30 min at 37 °C. Pancreatic lipase activity was determined by measuring the hydrolysis of p-nitrophenyl butyrate to p-nitrophenol at 405 nm using a UV-visible spectrophotometer. DMSO was used as negative control while Orlistat was used as a positive control. The inhibitory activity (%) was calculated according to the following formula:

% Inhibition = [(OD CONTROL-OD SAMPLE)/OD CONTROL] x 100

3. Results and Discussion

For comprehensive metabolic profiling of the seventeen acquired myrrh samples, a multiple array pattern of experimentally designed techniques was implemented, ranging from simple physical attributes passing through spectroscopic techniques ending with separating chromatographic analysis.

3.1. *Determination of particles RGB values of the intact samples' images*

The color of the samples (RGB) was chosen to reflect the sample's color variation into numerical values and values obtained mentioned in the supplementary material.

In order to translate the samples' colors into numerical values, the entire samples' images were analyzed separately using imageJ software the average values of Red (R), Green (G) and Blue (B) for each particle are recorded in table 1. RGB stands for red, green and blue channels measured as pixels, starting with black color first and changes according to light emitted. For examples 24-bit color image, white color measured as R255, G255, B255; black color: R0, G0, B0. Pure red color: R255, G0, B0, green color: R0, G255, B0, blue color: R0, G0, B 255. The histogram is calculated by converting each pixel to grayscale using the formula gray=0.299red+0.587green+0.114blue (Mahgoub et al., 2020). These three colors are the main color contributing in the other colors and as a result all colors can be detected in pixels and split into three main

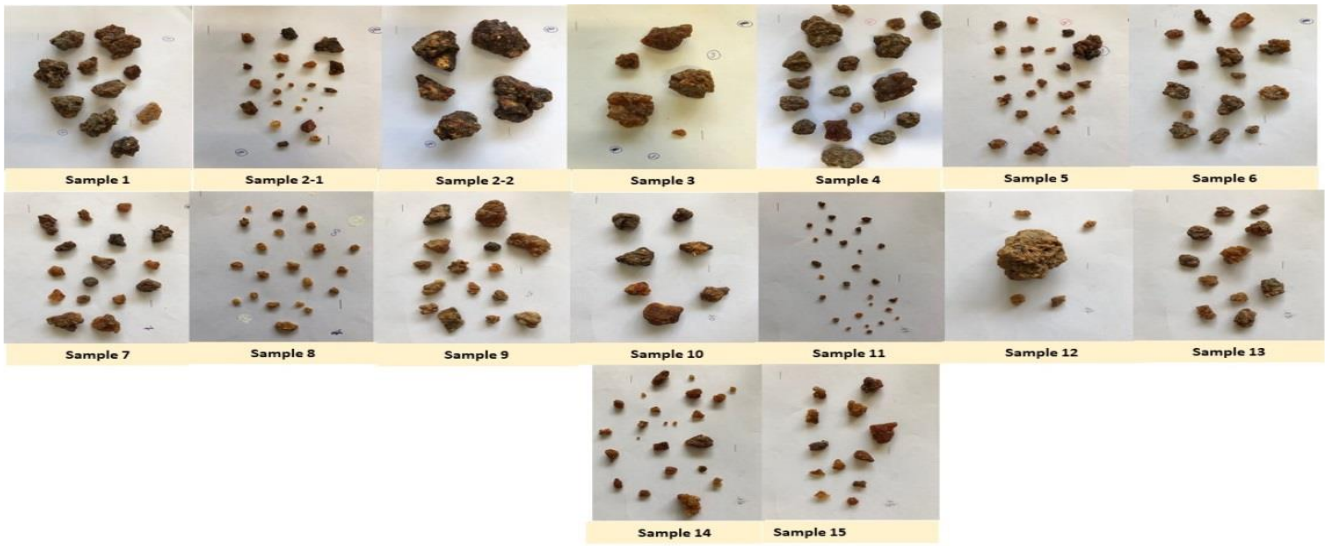

Figure 1: photo of 15 myrrh samples

channels. For example, sample 1 red: 207.31, green: 160.1 and blue :16.9, which means that red is the maximum, blue minimum and green is the medium color contribution in the whole color, resulting in a shade of orange color. When we review the results obtained from physical examination of the collected samples (Fig. 1 and 2), obviously, particle size does not stand by itself for any qualitative or quantitative analysis however, it might reflect or throw light on shipping, storage or post harvesting processes. (Table 2)

Table 2: Intact samples' particle size

Sample number	Average length (cm)	Range of particles length (cm)
sample 1	3.39	2.55-4.49
sample 2-1	0.89	0.34-1.88
sample 2-2	4.88	4.09-5.43
sample 3	3.03	1.74-3.86
sample 4	2.76	1.29-4.32
sample 5	0.95	0.69-1.128
sample 6	1.44	0.83-2.08
sample 7	1.69	1.12-2.17
sample 8	0.85	0.62-1.28
sample 9	2.05	1.16-3.14
sample 10	2.44	1.86-3.08
sample 11	0.55	0.44-0.69
sample 12	7.04	One large piece and few small from 1-7
sample 13	1.92	1.53-2.22
sample 14	0.96	0.36-2.08
sample 15	1.47	0.99-2.46
sample 16	0.52	0.41-0.71
sample 17	0.66	0.51-0.87

Table 3: Average RGB values of the myrrh samples

Sample number	Red	Green	Blue	Intensity
sample 1	79.7	59.2	38.8	62.9
sample 2	74.8	41.2	20.3	48.9
sample 2 large	80.0	55.8	36.4	60.8
sample 3	86.7	54.2	25.4	60.6
sample 4	77.0	57.4	36.6	60.9
sample 5	97.2	57.7	33.7	67.3
sample 6	85.9	61.7	39.37	66.6
sample 7	102.3	64.5	34.0	70.8
sample 8	114.7	69.6	28.9	78.6
sample 9	117.0	79.0	44.6	87.1
sample 10	93.3	61.0	35.2	66.8
sample 11	66.1	35.9	18.4	43.0
sample 12	117.2	80.6	47.5	86.0
sample 13	92.3	61.9	38.7	68.3
sample 14	99.1	51.8	22.6	61.6
sample 15	104.8	55.8	25.2	67.1
sample 16	72.5	36.7	15.3	45.0
sample 17	82.7	30.6	13.3	44.1

Secondly, the color of the myrrh samples (Fig.2) might give us some ideas about age or geographical source and this was concluded from the PCA below (Table 3).

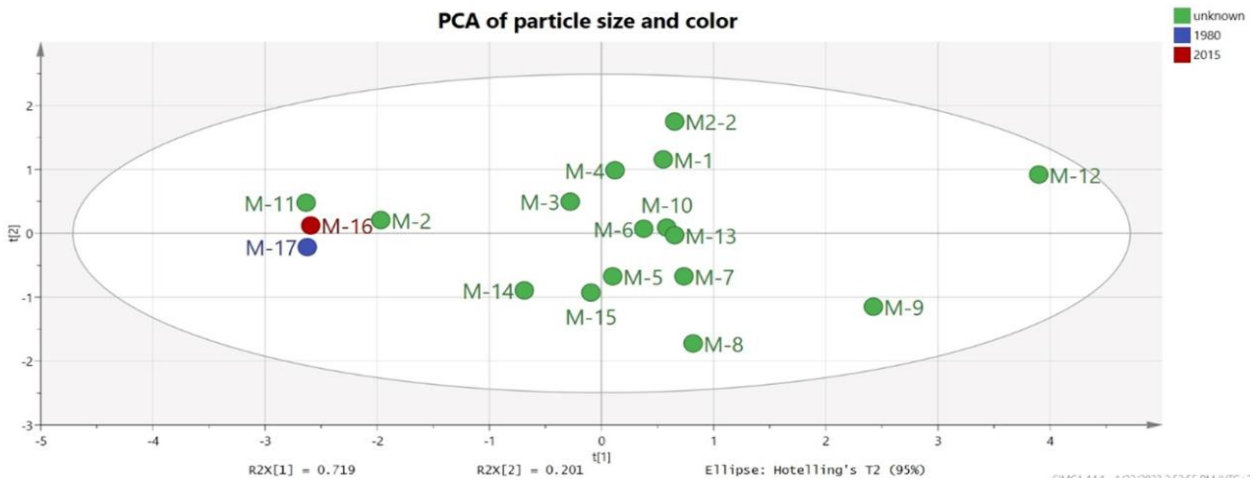

Figure 2 score scatter plot of PCA for size and RGB of particles.

We recalled the presence of two very old myrrh samples (16 and 17) from our departmental chemical depositoryas a 2nd sample tamplate. We concluded that pc2 is the coordinate reflecting sample color (age). Particle color is one of the main factors reflecting age.

We can conclude that myrrh contains some unstable materials which change by age to darker elements. A 3D of the mean centered RGB values of 5-8 representative particles from each sample could be related to the origin of the samples as shown in Figure 3.

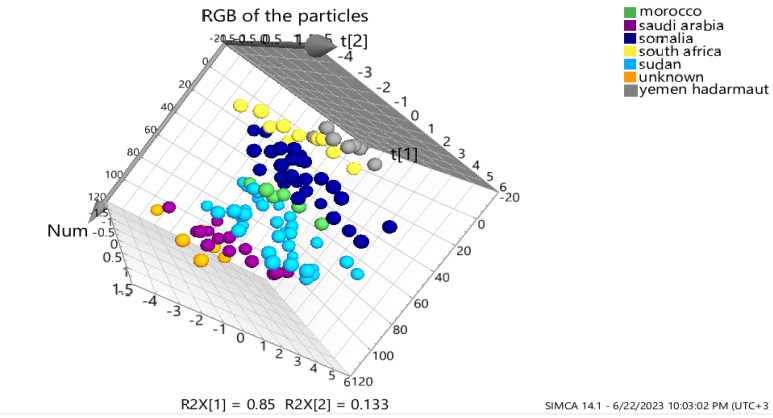

Figure 3: RGB of the particles related to the origin

3.2. Photographic analysis of myrrh sample solutions

Meanwhile the colors of the solution might confirm the above mentioned results as methanolic extracts. It was astonishing to observe that the colors of methanolic solutions of myrrh samples were widely different (Fig 4). Their color ranged from yellow to reddish orange as shown in figure 4 we measured RGB values for each solution (Table 4).

We designed a further experiment to find more specific validation, dissolving myrrh samples in methanol as a general solvent to explore the selectivity of the solvent to extract specific compounds, which will contribute in confirming the above-mentioned observation. Intentionally, we took pictures of the solution on a white background to measure color reflectance rather than light absorption. It was thought to explore the visibility of absorbing light to design such an experiment.

Table 4: Average RGB values of the myrrh samples solutions

Sample no.	red	green	blue	intensity
sample 1	207.31	160.1	16.9	157.918
sample 2	203.9	160.5	50.6	161.5
sample 3	211.8	193.9	116.7	190.5
sample 4	206.5	177	72.1	173.9
sample 5	201.2	142.4	3.9	144.2
sample 6	208.8	166.9	37.1	164.7
sample 7	199.6	171.3	92.1	170.8
sample 8	201.6	127.6	2.2	135.4
sample 9	207.9	167	50.6	165.9
sample 10	205.6	157.9	23.2	156.8
sample 11	166.5	75.7	18.3	96.2
sample 12	206.3	163.6	41.1	162.4
sample 13	203.8	142.1	1.8	144.6
sample 14	208.7	159.2	13.5	157.4
sample 15	210.4	164.2	26.1	162.2

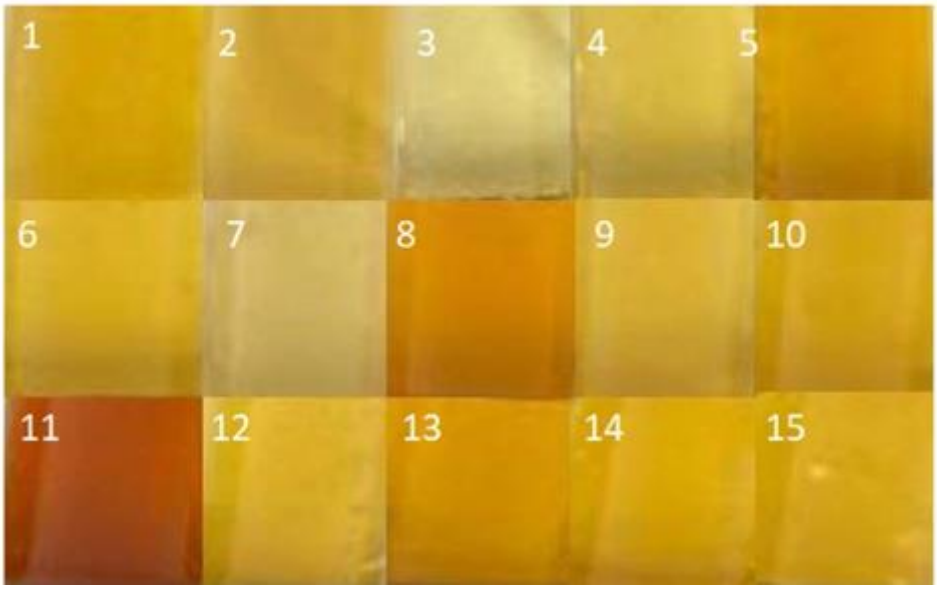

Figure 4: photo of methanolic myrrh samples' solutions

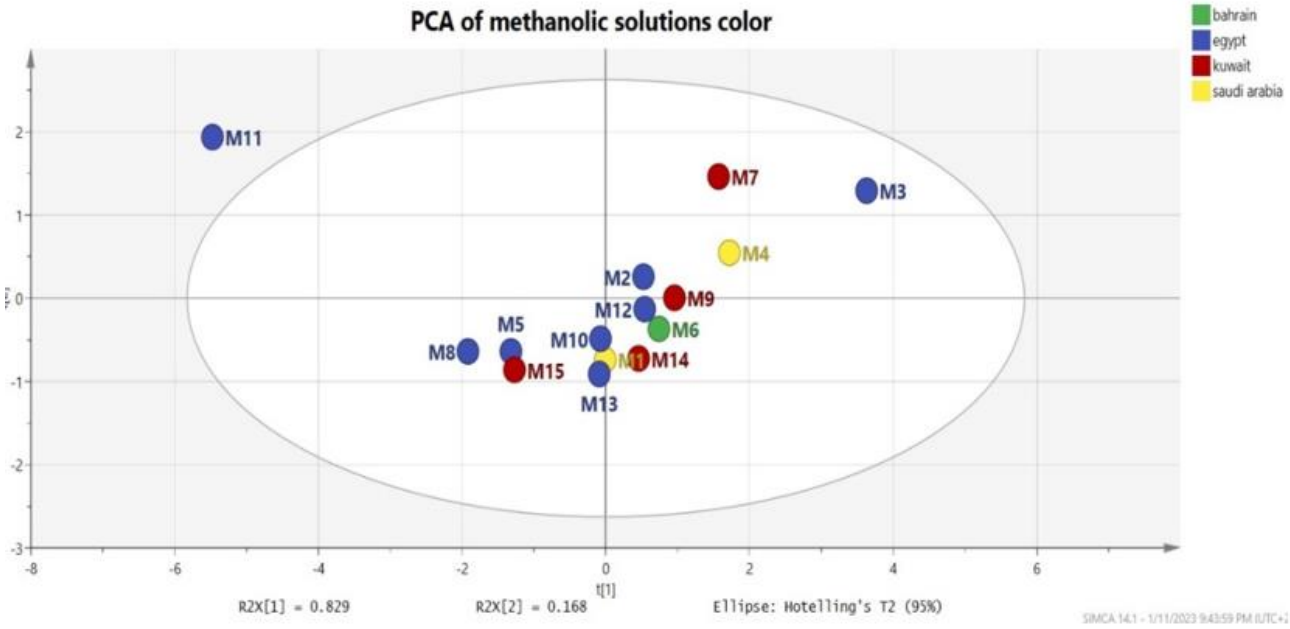

Figure 5: PCA score scatter plot RGB image color analysis of methanolic solutions.

From PCA score scatter plot (Fig.5) we noticed that all samples were clustered around pc1and pc2 except for samples 11 on the upper left quarter which was the darkest methanolic solution obtained and samples 7, 3, 4 on upper right quarter which was the lightest extract obtained (least absorbed solution). From the data collected (Table S4) we figured that pc1 contributes to the green variable while pc2 to the blue variable. This in conclusion showed that the major color contributed to the change was the blue color and its dilution (green color).

3.3. HPTLC analysis of myrrh samples

Here by, thin layer chromatography stands as a very simple technique, yet of great importance. Obviously, TLC can produce a profile of material used, specially that myrrh is almost like a purified extract (exudate). Which explain Constitution variability in compositional analysis, variation domain. Data of plate was acquired and numerically evaluated using image j software.

TLC was analyzed using two approaches based on the wisdom of the methodology, using two revealing agents; anisaldehyde as a general revealing agent while methanol/sulphuric was more specific in detecting fluorescents compounds in a qualitative approach (Figure 6, 7)

For imagej we adopted also two trials, first one with analyzing the plate into three different channels blue, green and red ones (Figure 10-12) and the second analyzing the individual spots presenting each component of the mixture into its RGB components using the rectangle marker in the toolbar to define the spots manually (Figure 8).

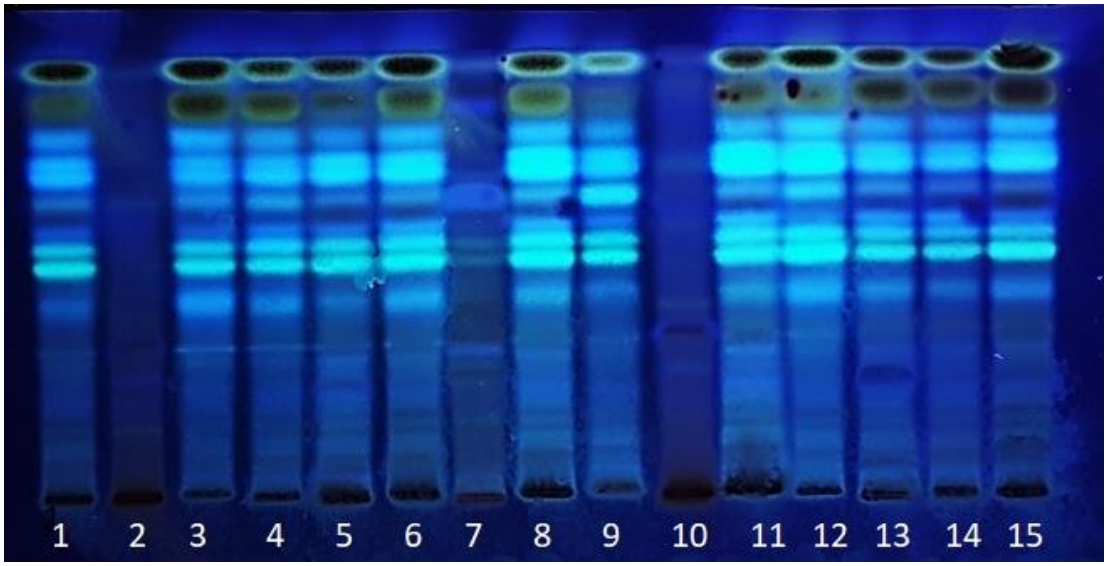

Figure 6: TLC of myrrh samples after spraying with methanol /sulphuric acid reagent and visualization under UV light at λ 366 nm.

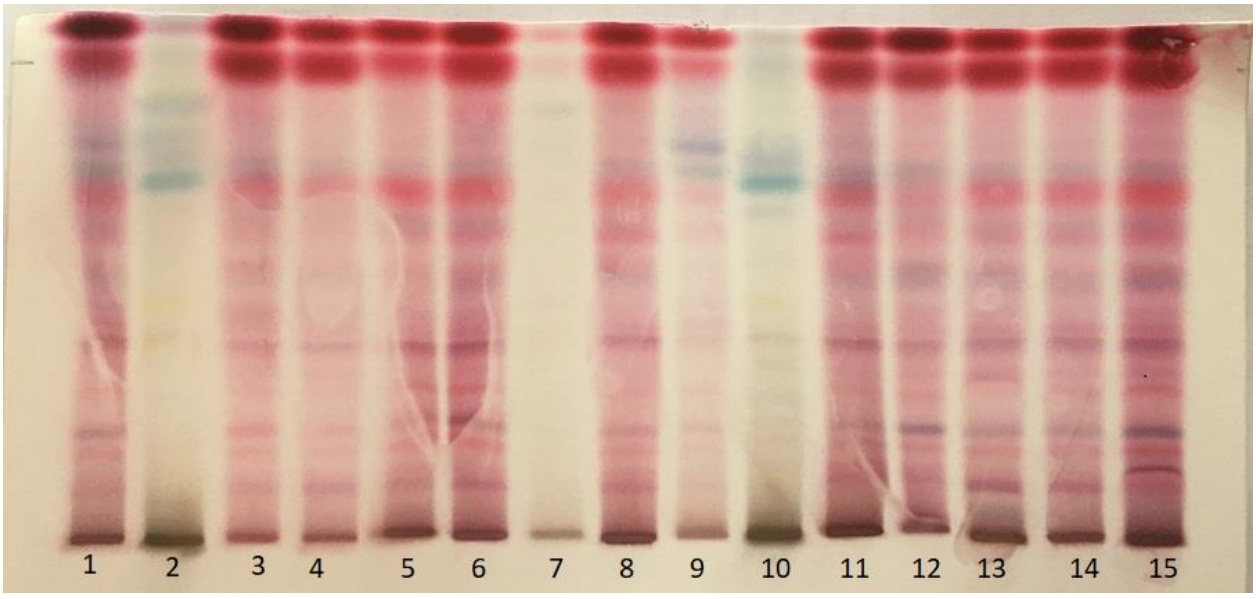

Figure 7: TLC of myrrh samples after spraying with anisaldehyde /sulphuric acid reagent and visualization under day light.

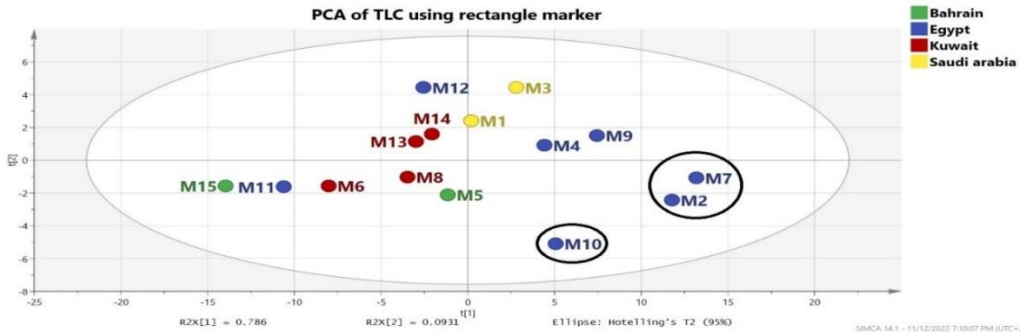

Figure 8: PCA scatter plot for TLC spot analysis via imagej

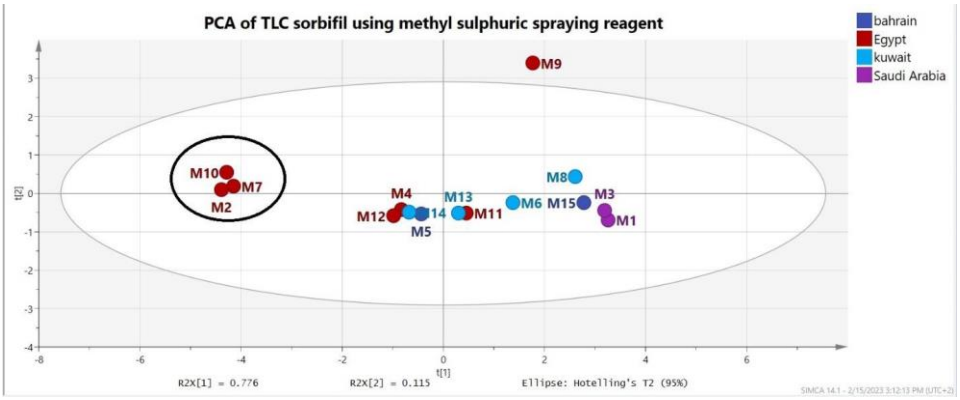

Figure 9: PCA scatter plot for TLC spot analysis using methanol sulfuric revealing agent

The most common characteristic features of most of the samples was the presence of seven luminous blue spots at R_f of 0.47,0.57,0.6,0,62,0.81,0.87, and 0.9., in addition to two teal-colored ones 0.42,0.44 the least polar constituents were concentrated as two major spots at the solvent front. In addition to some retained compounds on the starting line.

Moreover, post chromatographic derivatization with a coloring agent anisaldehyde /sulphuric acid reagent figure 7 exposed different shades of pink, purple to violet- colored spots which might indicate the presence of sesquiterpenes known to be present in myrrh extract. Further analysis is recommended to find a complete profile for myrrh.

TLC PCAs of all methods tried (sorbfil and imagej) figure 8-12 showed clustering of samples 2,7,10 which are different in pattern than the rest of the samples and it was obvious on the TLC plate itself. However, it looks like samples were grouped according to supplier.

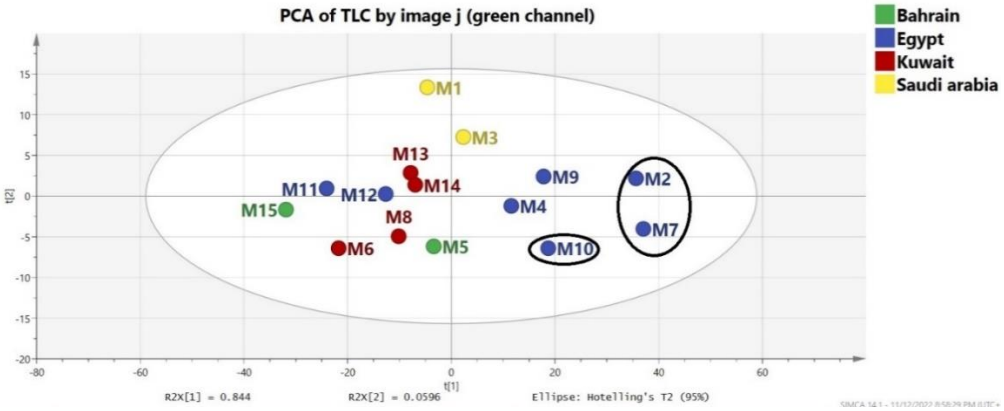

Figure 10: PCA scatter plot for TLC spots analysis via imagej (green channel)

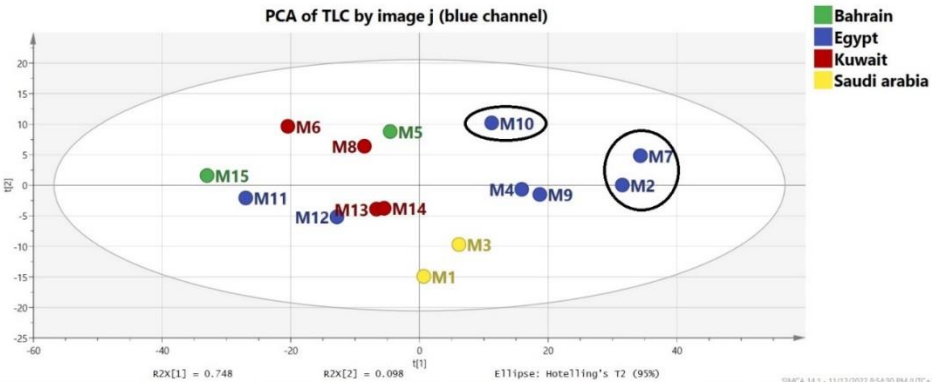

Figure 11: PCA scatter plot for TLC spots analysis via imagej (blue channel)

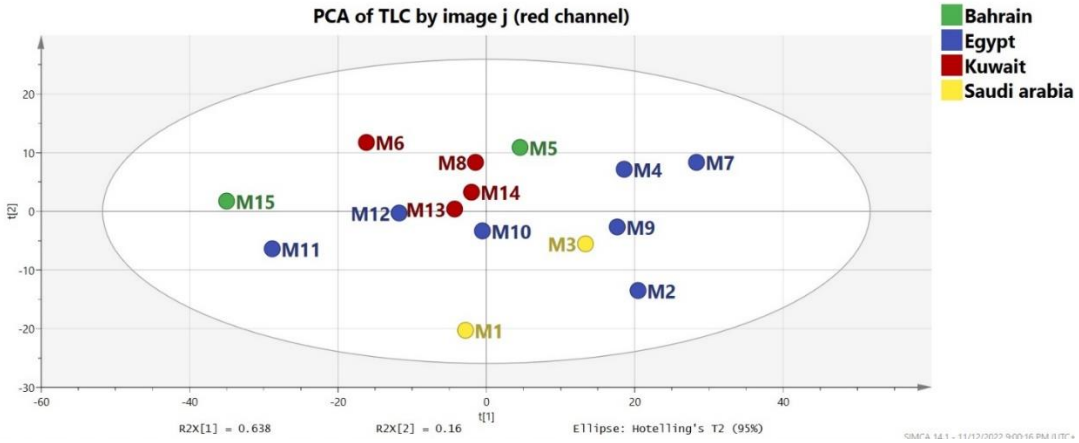

Figure 12: PCA scatter plot TLC spots analysis via imagej (red channel)

3.4. PLS regression of TLC and alpha glucosidase inhibition

PLS of TLC (figure 13) suggested 3-4 violet spots to be the important variable in alpha glucosidase inhibition and the starting line to be the least contributed, which is in agreement with the previously reported docking studies which suggested several sesquiterpenes along with some components of the resin part to be responsible for the activity[(Al-Radadi, 2022)

Although TLC might be very exclusive in establishing the chemical constitution or similarities or differences off the compositional profile of each sample yet spectroscopic methods might much easier or faster in expressing similarities or differences between samples in each content of functionalities and structural variation.

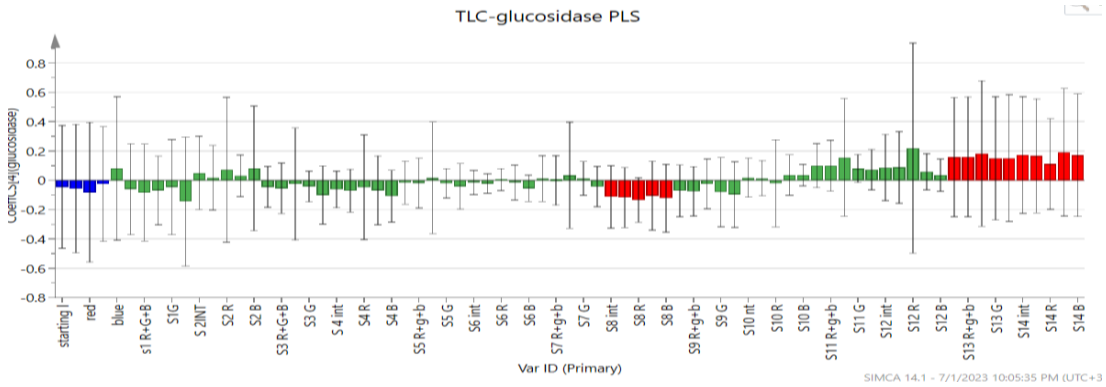

Figure 13: TLC-glucosidase PLS

3.5. NIR spectroscopic analysis

NIR analytical technique was used to examine major and gross components of myrrh samples,

In our study the measurements were performed three times on same samples selected from different sites of each specimen to assess the homogeneity among the measured data. As we can see in figure 14, a good reproducibility was observed for the spectroscopic data for the investigated specimens.

NIR spectra of Myrrh has been previously described by Hollein (Hollein et al., n.d.)in a short poor study which purpose was just to discriminate Myrrh amongst 14 chemically unrelated herbs.

As Myrrh chemistry is complicated, a tentative assignment of the peaks can be illustrated as :8802-8007 cm−1 –CH3 second overtone including 8264 C-H stretch second overtone of CH2 of arabinose and galactose 7197-6503 –CH2 combines region –OH stretching 1st overtone of the sugar moieties (Mahgoub et al., 2020) C=O of glucuronic acid (Dong et al., 2017)third overtone in addition to methylene, methyl C–H stretch and bending combination (2nd overtone and 2nd combination bands(Kuriakose & Joe, 2013) , 5994-5600 symmetric and asymmetric CH2 stretching, the –CH aliphatic 1st overtone of the sugar moiety, 5299-4998 carbonyl or water, 4991-4520 –CH=CH, 4512-4212 –CH3 combination , 4204-3857–CH2 combination.

Sesquiterpenes like furanoeudesma-1,3-diene, curzerenone display overtones bands of symmetric and asymmetric CH2 stretching in the region 5800–5700 cm−1. The second overtone of the lactone carbonyl group is usually observed in the region 5400–5100 cm−1, while the overtone of C–O stretching is observed near 4700 cm−1 and C–H bending vibration is displayed around 4300 cm−1 (Mahgoub et al., 2020)].

Upon close examination of the spectra of the 15 samples (figure 14), we can clearly notice that Sample 7 and 10 was different in the region 3700-4400, 4550-4800 and 5600 -6200 cm−1 while 12 was different in the region 3700-4400, and 5600-6200 cm−1. That was also reflected in the PCA scatter plot (fig 15). As the PCA score plot of the NIR spectra of the myrrh samples correlate it to the area of collection except for the sample 12, this can be explained that there may be several factors contributing in the clustering of the samples which can be the age of the samples or their grade.

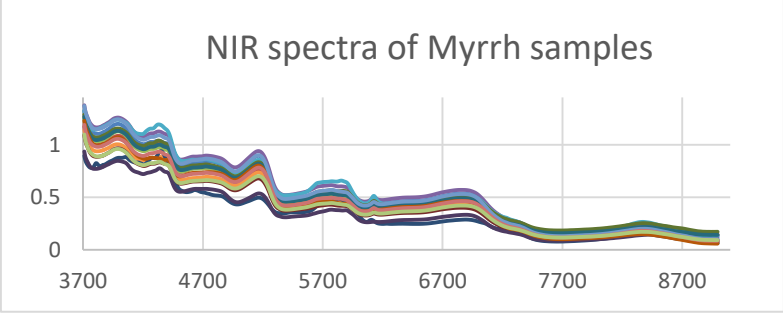

Figure 14: NIR spectra of myrrh samples

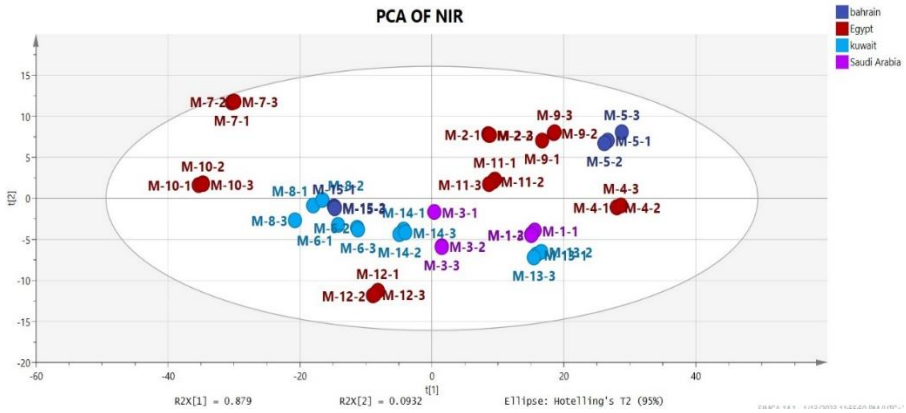

Figure 15: score scatter plot of first two PCA components of NIR spectra of all Myrrh samples.

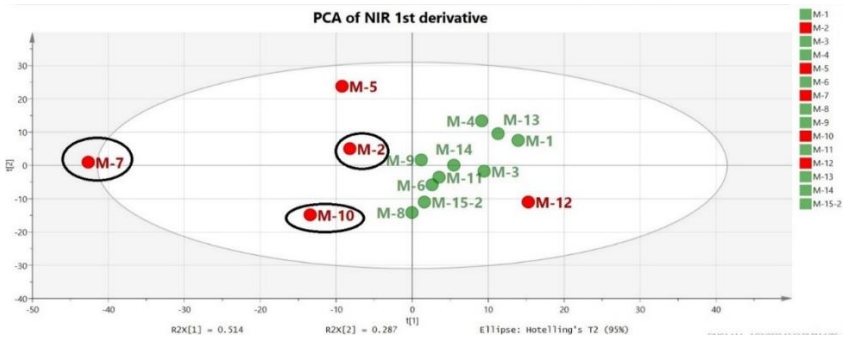

Figure 16: PCA scatter plot of first derivative of NIR spectra.

A model was constructed using the first derivative of the NIR spectrum, the PCA of the first two components (fig 16) showed a clustering of almost all samples except for samples 2, 5 ,7, 10 and 12 which have been previously indicted by TLC of their poor relation of the composition to other samples. This has been further confirmed in the PCA of 1st derivative (fig. 16) where data processing (1st derivative) was quite helpful in resolving these three samples from the pattern of the other samples. A conclusion that was evident from the TLC in both revealing agents and also samples 2, 7 and 10 have low absorbance in NIR spectrum fig. 14.

A PCA model was constructed based on the absorbance of only the seven peaks. Peak 1 (8802-8007) cm^{-1}, peak 2 (7197-6503) cm^{-1}, peak 3 (5994-5606) cm^{-1}, peak 4 (5299-4998) cm^{-1}, peak 5 (4991-4520) cm^{-1}, peak 6 (4512-4212) cm^{-1} and peak 7 (4204-3857) cm^{-1}. The average absorbance for each of these regions was calculated individually P_n, then a ratio was calculated as P_1/P_2, P_1/P_3, P_1/P_4, P_1/P_5, P_1/P_6, P_1/P_7. and similarly repeated for each of the peaks. These 7 values were arranged in a matrix for all the samples and used to build a model.

A further elaboration on data obtained from NIR is performed by calculating the relative ratios of absorbances' peaks to total peaks (P_n/P_x). figure 17-18. Surprisingly P_4/P_x was the only peak ratio adequate to clarify the difference between samples 2, 7 and 10 as illustrated in TLC model. Consequently, this region might indicate absorbances of compounds that might be lacking in samples 2, 7 and 10.

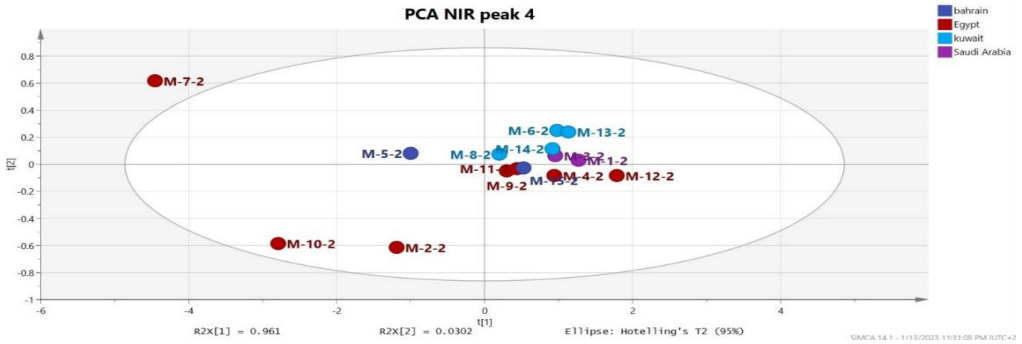

Figure 17: PCA scatter plot of peak 4 (P_4/P_x) ratio.

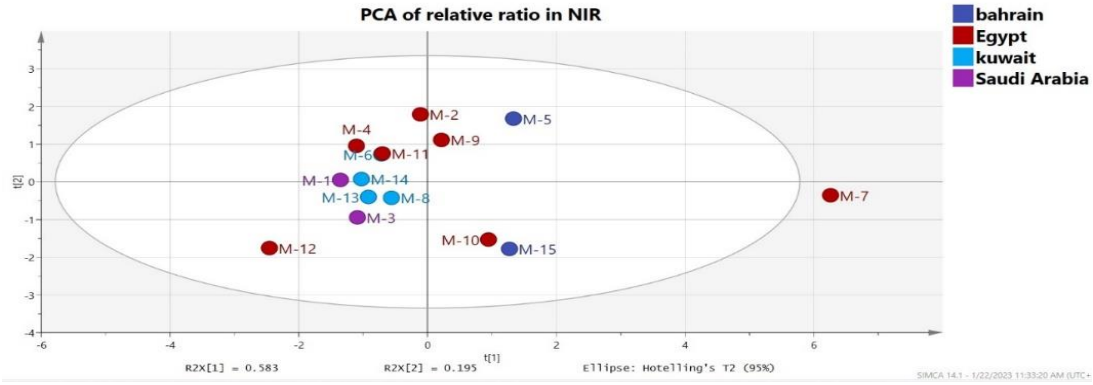

Figure 18: PCA scatter plot of NIR all (P_n/P_x) peak ratios

Likewise, the relative ratio of reflectance peaks to the total reflectance was quite similar to the above-mentioned discussion.

3.6. UV spectroscopic analysis

UV spectroscopic analysis is capable of mining for the chromophoric attributes from a wide array of others. Different approaches were tried in order to attain conclusive remarks about the measured samples. The first approach was choosing the entire UV variables from 250 to 350 nm, the second one was to select more than one region (290-299), (280-289) and (279-260). Thirdly, the peak ratio of absorbance peaks method (Pn/Px) as illustrated previously in NIR technique (figure 20-21). Moreover, aluminum chloride shift reagent spectra were utilized to unravel extra-features of myrrh samples such as the presence of ortho-dihydroxy groups (fig19).

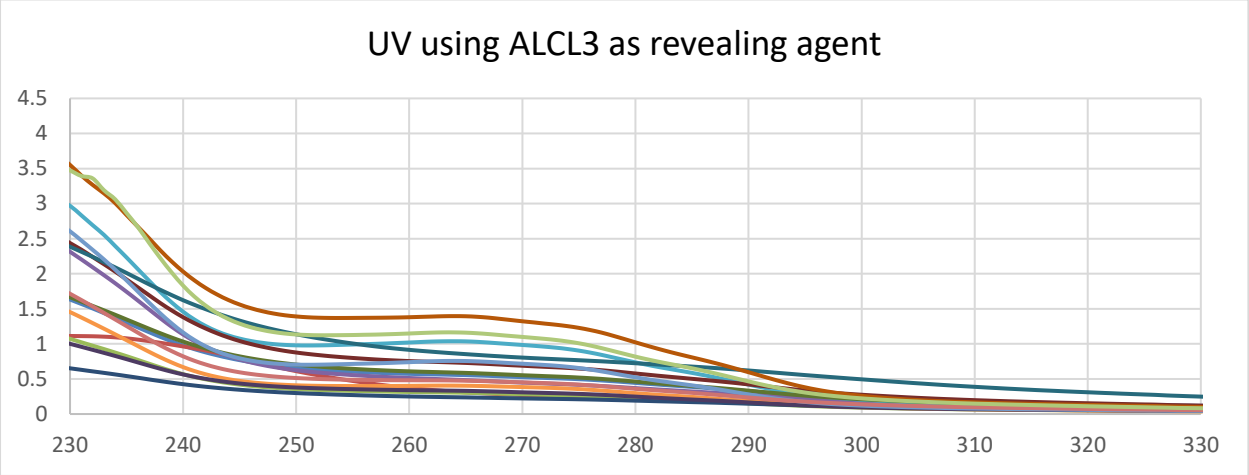

Figure 19: UV spectra using ALCL3 as revealing agent

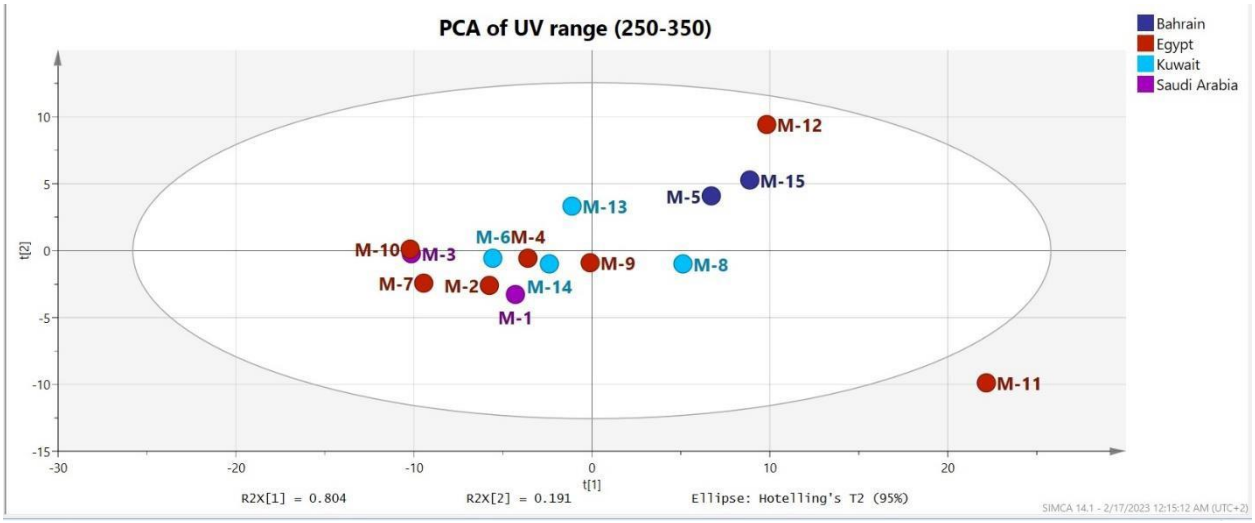

Figure 20: PCA scatter plot of UV variables ranging from 250 to 350 nm.

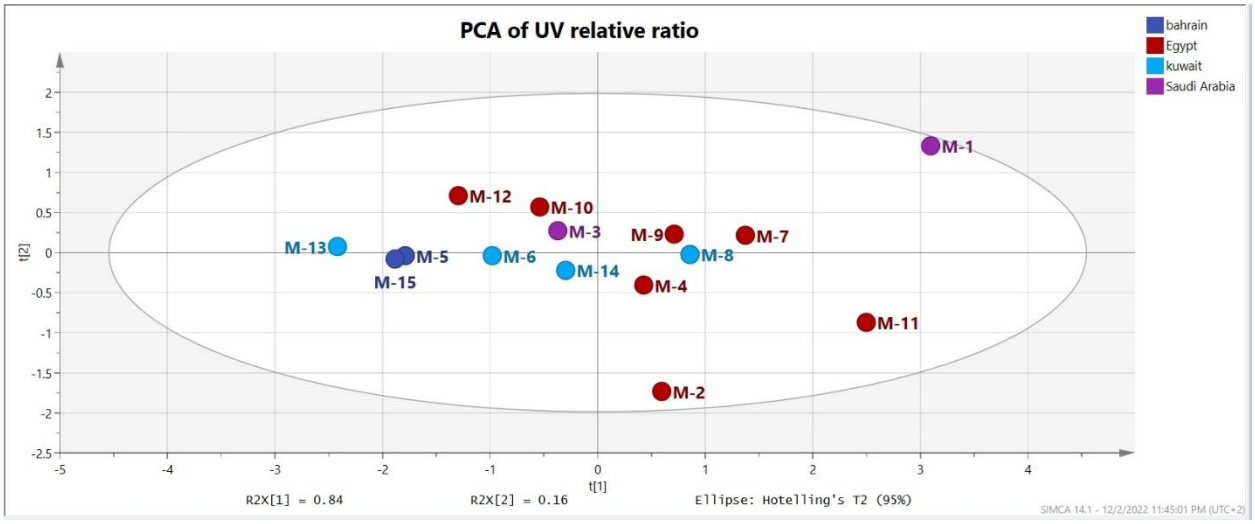

Figure 21: PCA scatter plot for UV relative ratio (Pn/Px).

Obviously, UV showed difference between samples 5,8,11,12,13,15 and the rest in conjugated systems with significant absorbances. Remarkably sample 11 which was estimated to be an old-aged sample after observing the color of solution, was in parallel clear in all UV PCAs away from the clustered samples.

3.7. *In vitro* evaluation of some selected biological activities of myrrh

Myrrh possesses a wide array of biological properties such as antibacterial, antifungal and antiviral against vast of microorganisms. Moreover, a recent research article revealed great anti-inflammatory, lipase inhibitory, anti-diabetic as a well as cytotoxic activity of gold-conjugated polyphenol nanoparticles of myrrh (Al-Radadi, 2022). This has promoted us to investigate the effect of geographical origin on these activities whenever possible.

3.7.1. In vitro α-glucosidase inhibitory activity assay

Alpha-glucosidase inhibitors (AGIs) are well known drugs used widely in management of hyperglycemia in patients with type 2 diabetes mellitus. Prescribed by physicians to patients, especially those who are at risk of lactic acidosis and those who can suffer from hypoglycemia as a side effect of some other antidiabetics, such as sulfonylureas and metformin (Moelands et al., 2018). Some clinical studies showed positive results on type 1 diabetes mellitus as well. An off-side label use of acarbose (AGIs) was as weight loss pills (Nakhaee & Sanjari, 2013).

The average ic50 value of the myrrh samples was 55.39 ± 7.34 which was average regarding acarbose as an **α**-glucosidase inhibitor. Samples 1,7,8 and 14 showed the highest activity. On the other hand, no clear correlation can be made between α-glucosidase inhibitory activity and the country of purchase or the claimed origin.

A previous study on molecular docking of several compounds of myrrh showed that the compound with the highest binding inhibitor was 3,4,4-trimethyl-3-(3-oxobut-1-enyl)bicyclo(4,1,0)heptan-2on(Al-Radadi, 2022).

3.7.2. PLSR model for α-glucosidase inhibitory activity prediction

3 acquisitions from each sample with a total of 45 samples was prepared, their NIR spectra was recorded as well as their alpha glucosidase inhibitory activity. The data was divided 40 samples to construct the calibration model and 5 to construct the prediction model. The resulted PLS model was validated using R2 as an indicator of data fitting in addition to observed versus predicted plots and root mean square error of calibration (RMSEC). The model was also validated using external prediction set.

The important zones in NIR spectra of Myrrh that contribute to the observed alpha glucosidase activity were identified using the coefficient plots (Fig. 22).

8430-8300 (the second overtone of CH stretching vibrations at 8300 cm^{-1} that corresponds to methyl (-CH_3), methylene (-CH_2), and olefin (-CH=CH-) bonds(Grassi et al., 2021)7367-7320 , 7250-7220 assigned to the C–H stretching vibration,(Bai et al., 2023), or CH in plane bending and ring in plane bending.6009-5900, 5800-5815, 5690, 5560, 5530-5360, 5250-5040,

5000-4820 (C=O stretching) (Grabska et al., 2021)

4400-4370, 4310-4280 represent CH and CH2 s overtones3920-3800

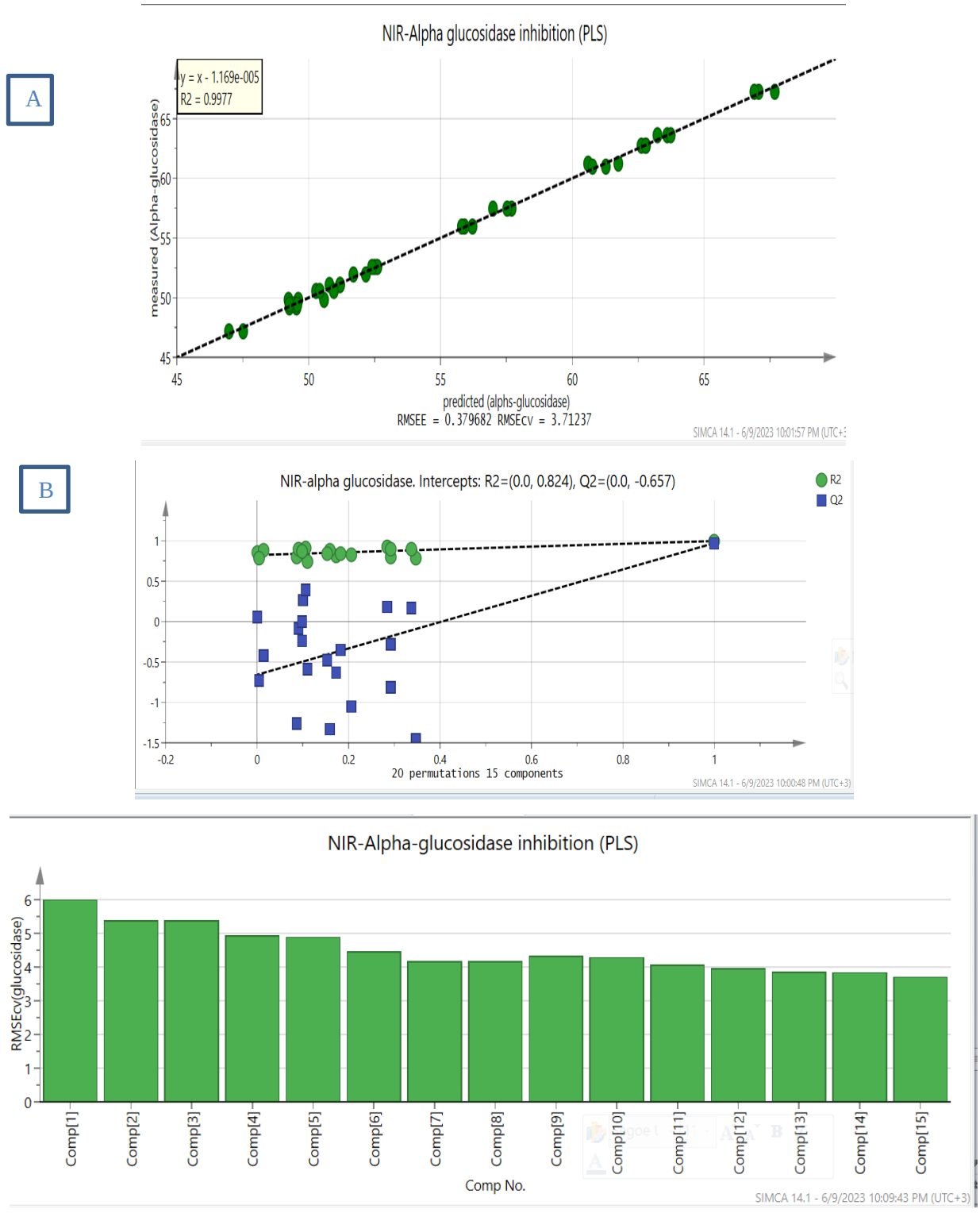

Figure 22: Validation for PLSR model of Myrrh samples represented by: (A) the relationship between observed and predicted values, (B) permutation plots, (C) correlation between RMSECV and PLSR optimal latent variables.

A VIP plot showed the importance of the variable in descending order (Fig. 22) A VIP score of 0.9 was chosen as a threshold value for the variables that significantly contribute to accurate prediction. Then a PLSR model was constructed using the selected variables with VIP scores higher than 0.9 (Fig. 23). The criteria to judge the model: R2 , RMSEC, RMSECV, and RMSEP values as well as the intercept values of permutation plots clearly show that the PLSR models were improved after removing noninformative spectral variables which affect the precision and robustness and may have resulted from noise, baseline variation, as well as chemical and physical interferences.

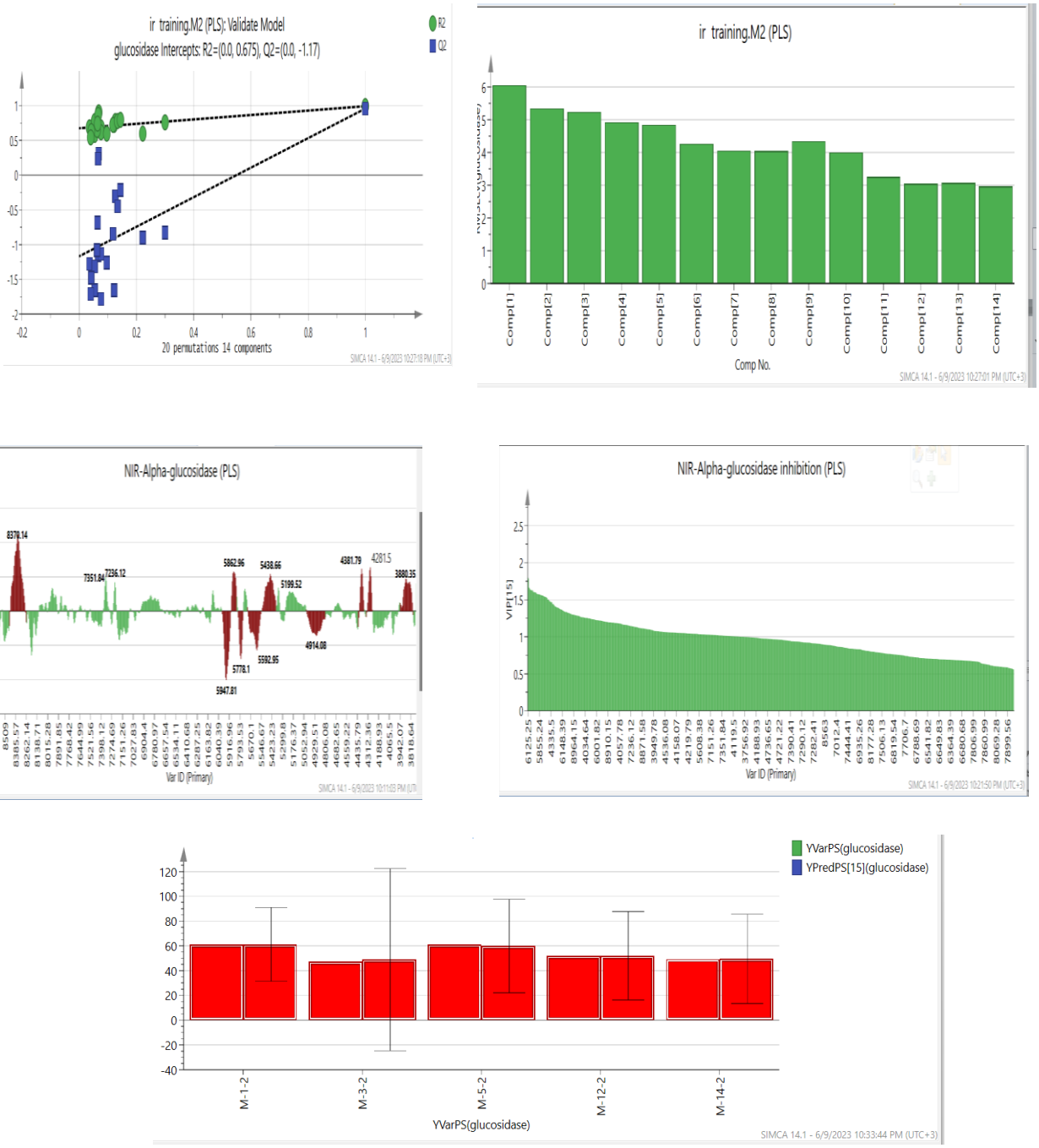

Figure 23: NIR alpha glucosidase (PLS)

Conclusion:

Most of the previous research done on myrrh were directed to explore the chemical constituents and hence biological activity that might be what claimed to be as myrrh. so far, the exact chemical constitution (metabolic profile) of what is called myrrh is not defined. All literature discussing myrrh relate the product to many different species which under the current understanding of metabolomics might not be true.

After resolving all analytical methods, none of the commercial samples obtained a common profile, which put the market under suspicion of proposing proper attributes of myrrh.

Variable sources and reported adulteration encounters of myrrh is a challenging problem. In order to secure the highest quality and the authenticity of the available market commodities, which in return will be a concern for the efficacy of the oleogum resin. Moreover, considering the current high price of myrrh made it more liable to adulteration.

In this study, NIR spectra of Myrrh were recorded and attempt to assign the peaks to its content this is the first study to use this approach for myrrh.

The results shown are preliminary and we recommend the use of larger number of samples of myrrh of known species and/or origin to obtain more robust models for the analysis of unknown samples.

Declarations

Consent for publication

Not applicable.

Availability of data and materials

The datasets used and/or analysed during the current study are available from the corresponding author on reasonable request.

Competing interests

The authors declare that they have no competing interests.

Funding

This study was partially funded by Alexandria University.

Authors' contributions

MI, HF, RI suggested the study design and methodology. YA collected the samples, performed the analyses. YA, HF conducted the multivariate data analysis and chemometric models. All authors contributed to interpretation of the results. All authors contributed to writing the manuscript and approved the final version.

Acknowledgements

The authors would like to thank Dr. Eva Edward lecturer of microbiology, faculty of pharmacy for carrying out the antifungal assay, and Dr Hala Shafik lecturer of industrial pharmacy, faculty of pharmacy for designing and carrying out a method for solubilization of myrrh in water.

References:

Al-Radadi, N. S. (2022). Single-step green synthesis of gold conjugated polyphenol nanoparticle using extracts of Saudi's myrrh: Their characterization, molecular docking and essential biological applications. *Saudi Pharmaceutical Journal : SPJ*, *30*(9), 1215. https://doi.org/10.1016/J.JSPS.2022.06.028

Alyafei, N. (2020). Can Myrrh Combat COVID-19? *Iberoamerican Journal of Medicine*, *00*, 223–229.

Assimopoulou, A. N., Zlatanos, S. N., & Papageorgiou, V. P. (2005). Antioxidant activity of natural resins and bioactive triterpenes in oil substrates. *Food Chemistry*, *92*(4), 721–727. https://doi.org/10.1016/j.foodchem.2004.08.033

Bai, X., Xu, Y., Chen, X., Dai, B., Tao, Y., & Xiong, X. (2023). *Analysis of Near-Infrared Spectral Properties and Quantitative Detection of Rose Oxide in Wine*. https://doi.org/10.3390/agronomy

Barakat, R., Elmorshedy, H., & Fenwick, A. (2005). Efficacy of myrrh in the treatment of human Schistosomiasis mansoni. *American Journal of Tropical Medicine and Hygiene*, *73*(2), 365–367. https://doi.org/10.4269/ajtmh.2005.73.365

Cao, B., Wei, X. C., Xu, X. R., Zhang, H. Z., Luo, C. H., Feng, B., Xu, R. C., Zhao, S. Y., Du, X. J., Han, L., & Zhang, D. K. (2019). Seeing the unseen of the combination of two natural resins, frankincense and myrrh: Changes in chemical constituents and pharmacological activities. In *Molecules* (Vol. 24, Issue 17). MDPI AG. https://doi.org/10.3390/molecules24173076

Chandrasekharnath, N., Mahlakshmi, Y. V, Jayalakshmi, L., Venkanna, B., & Uma, A. (2013). Screening and isolation of bioactive factors from Commiphora myrrha and evaluation of their antimicrobial activity. In *International Journal of Engineering Research and Applications (IJERA)* (Vol. 3). www.ijera.com

Dong, Y., Sørensen, K. M., He, S., & Engelsen, S. B. (2017). Gum Arabic authentication and mixture

quantification by near infrared spectroscopy. *Food Control*, *78*, 144–149. https://doi.org/10.1016/J.FOODCONT.2017.02.002

Grabska, J., Beć, K. B., Ozaki, Y., & Huck, C. W. (2021). Anharmonic dft study of near-infrared spectra of caffeine: Vibrational analysis of the second overtones and ternary combinations. *Molecules*, *26*(17). https://doi.org/10.3390/molecules26175212

Grassi, S., Jolayemi, O. S., Giovenzana, V., Tugnolo, A., Squeo, G., Conte, P., De Bruno, A., Flamminii, F., Casiraghi, E., & Alamprese, C. (2021). Near infrared spectroscopy as a green technology for the quality prediction of intact olives. *Foods*, *10*(5). https://doi.org/10.3390/foods10051042

Hamad, G. M., Taha, T. H., Alshehri, A., & El-Deeb, N. M. (2017). Myrrh as a Functional Food with Therapeutic Properties Against Colon Cancer in Traditional Meals. *Journal of Food Processing and Preservation*, *41*(1). https://doi.org/10.1111/jfpp.12963 Hanuš, L. O., Řezanka, T., Dembitsky, V. M., & Moussaieff, A. (2005). *MYRRH-COMMIPHORA CHEMISTRY*.

Hollein, M., Republic, C., & Strother, T. (n.d.). *Classification of herbs by FT-NIR spectroscopy Application note Authors*.

Kuriakose, S., & Joe, I. H. (2013). Feasibility of using near infrared spectroscopy to detect and quantify an adulterant in high quality sandalwood oil. *Spectrochimica Acta Part A: Molecular and Biomolecular Spectroscopy*, *115*, 568–573. https://doi.org/10.1016/J.SAA.2013.06.076

Mahgoub, Y. A., Shawky, E., Darwish, F. A., El Sebakhy, N. A., & El-Hawiet, A. M. (2020). Near-infrared spectroscopy combined with chemometrics for quality control of German chamomile (Matricaria recutita L.) and detection of its adulteration by related toxic plants. *Microchemical Journal*, *158*, 105153. https://doi.org/10.1016/J.MICROC.2020.105153

Massoud, A. M. A., El-Sherbini, E. T., Mos-Tafa, N., Saleh, K., Fathy Abouel-Nour, M., & Morsy, A. T. A. (2010). MIRAZID IN TREATMENT OF THREE ZOONOTIC TREMATODES IN BENI-SWEIF AND DAKHALIA GOVERNORATES. In *Journal of the Egyptian Society of Parasitology* (Vol. 40, Issue 1). http://www.docudesk.com

Miller, J. M., & Goodell, H. B. (1968). Frankincense and myrrh. *Surgery* Gynecology and Obstetrics, 127(2), 360–365. https://doi.org/10.2307/3209285

Moelands, S. V. L., Lucassen, P. L. B. J., Akkermans, R. P., De Grauw, W. J. C., & Van de Laar, F. A. (2018). Alpha-glucosidase inhibitors for prevention or delay of type 2 diabetes mellitus and its associated complications in people at increased risk of developing type 2 diabetes mellitus. The Cochrane Database of Systematic Reviews, 12(12). https://doi.org/10.1002/14651858.CD005061.PUB3

Nakhaee, A., & Sanjari, M. (2013). Evaluation of effect of acarbose consumption on weight losing in non-diabetic overweight or obese patients in Kerman. In Journal of Research in Medical Sciences.

Shameem, I. , & Fahad, T. (2018). Phytochemical & therapeutic potentials of Murr makki (Commiphora myrrha): A review PHYTOCHEMICAL AND THERAPEUTIC POTENTIALS OF MURR MAKKI (COMMIPHORA MYRRHA): A REVIEW Tooba Fahad*. https://www.researchgate.net/publication/329521561